Delay of HeLa Cell Cleavage into Interphase Using Dihydrocytochalasin B: Retention of a Postmitotic Spindle and Telophase Disc Correlates with Synchronous Cleavage Recovery

Stéphanie N. Martineau, Paul R. Andreassen, and Robert L. Margolis

Institut de Biologie Structurale–Jean-Pierre Ebel, 38027 Grenoble, France

Abstract. The molecular signals that determine the position and timing of the cleavage furrow during mammalian cell cytokinesis are presently unknown. We have studied in detail the effect of dihydrocytochalasin B (DCB), a drug that interferes with actin assembly, on specific late mitotic events in synchronous HeLa cells. When cleavage furrow formation is blocked at 10 μM DCB, cells return to interphase by the criteria of reformation of nuclei with lamin borders, degradation of the cyclin B component of $p34^{cdc2}$ kinase, and loss of mitosis specific MPM-2 antigens. However, the machinery for cell cleavage is retained for up to one hour into G_1 when cleavage cannot proceed. The components retained consist prominently of a "postmitotic" spindle and a telophase disc, a structure templated by the mitotic spindle in anaphase that may determine the position and timing of the cleavage furrow. Upon release from DCB block, G_1 cells proceed through a rapid and synchronous cleavage. We conclude that the mitotic spindle is not inevitably destroyed at the end of mitosis, but persists as an integral structure with the telophase disc in the absence of cleavage. We also conclude that cell cleavage can occur in G_1, and is therefore an event metabolically independent of mitosis. The retained telophase disc may indeed signal the position of furrow formation, as G_1 cleavage occurs only in the position where the retained disc underlies the cell cortex. The protocol we describe should now enable development of a model system for the study of mammalian cell cleavage as a synchronous event independent of mitosis.

During telophase, the terminating phase of mitosis, the cell cortex constricts inward at the position of the mitotic spindle equator, yielding two daughter cells. The process of cell cleavage thus represents the culmination of the mammalian cell cycle. Normally, the cleavage mechanism is precisely controlled to commence once the chromosomes have completed their poleward migration, but the specific proximal signals that control cleavage onset with such precise timing are not known. Indeed, despite its vital importance to the proper partitioning of chromosomes and of the cytoplasmic contents at the end of mitosis, the regulation and mechanism of cell cleavage are not well understood.

We have previously identified a late mitotic structure in mammalian cells, the telophase disc, which forms transiently in late anaphase at the site of the future cleavage event (Andreassen et al., 1991). The telophase disc appears to arise from proteins that are transported from the separating chromosomes during anaphase, which then migrate toward the equatorial position of the mitotic spindle. During late anaphase, the telophase disc expands from the mitotic spindle to the cell cortex at the position of the future cleavage furrow, until it bifurcates the cell (Andreassen et al., 1991). As cleavage progresses, the interpolar microtubules of the mitotic spindle disassemble toward the equatorial position of overlap between the two half spindles (Rattner, 1992). Finally, at the end of the cleavage process, the telophase disc and spindle microtubule remnants link the two daughter cells together in a midbody bridge (Andreassen et al., 1991; Rattner, 1992).

It has previously been demonstrated that the mitotic spindle is involved in determining the site of cleavage (Rappaport and Rappaport, 1974; Heidemann and Kirschner, 1975; Kawamura, 1977), which normally occurs at the position of the spindle equator. Given the close temporal and spatial association of the telophase disc with the site of the future cleavage furrow, we have proposed that the mitotic spindle communicates this information through the telophase disc that, once positioned by the spindle, then determines the site of cell cleavage (Margolis and Andreassen, 1993).

Although telophase is temporally coordinated to follow

Address correspondence to Robert L. Margolis, Institut de Biologie Structurale–J.P. Ebel, 41 avenue des Martyrs, 38027 Grenoble, France. Tel.: (33) 76 88 96 16. Fax: (33) 76 88 54 94.

previous steps in mitosis, and occurs in cells that are still morphologically mitotic by the criteria of containing condensed chromosomes and mitotic spindles, it is not apparent whether any telophase events are directly subject to mitotic control. Anaphase and telophase are not directly controlled by $p34^{cdc2}$ kinase activity. While $p34^{cdc2}$ is universally required to induce the onset of mitosis in eukaryotes (Nurse and Bisset, 1981; Nurse, 1990; Th'ng et al., 1990), it is abruptly inactivated at the onset of anaphase (Hunt et al., 1992; Holloway et al., 1993). We have here addressed the interdependency and the possible mitotic control of the different events in telophase by carefully examining the effect of inhibiting cleavage through use of dihydrocytochalasin B (DCB)[1]. DCB, a member of the cytochalasin family (Yahara et al., 1982), inhibits actin assembly in cells (Aubin et al., 1981) with a greater specificity than certain other cytochalasins (Atlas and Lin, 1978), and also interferes with the cell cleavage process (Atlas and Lin, 1978; Aubin et al., 1981; Andreassen et al., 1991).

In this study, we have found that reformation of interphase nuclei and the downregulation of mitosis-specific MPM-2 phosphorylation epitopes (Davis et al., 1983; Vandre et al., 1984) are not impeded by cleavage failure in the presence of DCB. However, the DCB-treated cells retain a persistent postmitotic spindle, which maintains its position between the two reformed nuclei and, in turn, the postmitotic spindle retains a telophase disc at its equator. We term this structure a "postmitotic spindle" because it has a spindle morphology clearly distinguishable from stembodies that are present in telophase cells, and because it is present in a cell that is largely interphase in character.

Our results suggest that the dissolution of the anaphase spindle and of the telophase disc are to some extent coupled to successful cell cleavage rather than being strictly coordinated with other events in mitotic exit. The persistence of these structures also suggests that they play a role in the cleavage mechanism. We define a cell as postmitotic when it has reconstituted interphase nuclei, but retains a spindle and telophase disc. A role for the postmitotic spindle and the telophase disc in cell cleavage is strongly supported by our finding that postmitotic cells synchronously cleave at the position of the telophase disc within minutes of the removal of DCB, but only if the cell's cortex maintains association with elements of the telophase disc.

Importantly, it now appears that cell cleavage is an event independent of mitotic control, and that it can be dissociated to occur in G_1. Additionally, postmitotic cleavage correlates well with the presence and position of both a persistent mitotic spindle and a telophase disc. Finally, as a result of our observations, we have shown that a synchronous system can be developed in which the control and mechanism of cell cleavage can be studied in a context that is independent of concurrent mitotic events.

Materials and Methods

Cell Culture and Synchronization

HeLa cells were cultured as monolayers in Dulbecco's Modified Eagle's Medium (GIBCO BRL, Paisley, UK) supplemented with 5% defined bovine calf serum (Hyclone, Logan, UT), and were kept in a humid incubator at 37°C with 5% CO_2.

Cells were grown on polylysine-coated coverslips for 48 h and were then treated for 12 h with 40 ng/ml nocodazole (Sigma Chem. Co., St. Louis, MO) to obtain a population arrested in mitosis. Progression in mitosis was initiated by washing with fresh culture medium (3 × 1 min each) and cells were then cultured in fresh medium either with or without 10 μM dihydrocytochalasin B (DCB; Sigma). At timepoints, cells were fixed in preparation for immunofluorescence microscopy.

Cells were recovered from treatment with DCB by washing with fresh medium (3 × 1 min) after exposure to DCB for varying times, depending upon the experiment.

Immunofluorescence Microscopy

For immunolocalization of all antigens except cyclin B and Eg5, cells were fixed 20 min at 37°C with 2% paraformaldehyde in PBS (136 mM NaCl, 2 mM KCl, 10.6 mM Na_2PO_4, and 1.5 mM KH_2PO_4 at pH 7.4). Cells were then permeabilized with 0.2% Triton X-100 in PBS for 3 min, and washed 5 min with PBS. Incubation with primary antibodies diluted in PBS containing 0.05% Tween-20 and 3% bovine serum albumin was for 60 min in a humid chamber. After three washes with PBS, cells were incubated for 30 min with secondary antibodies and subsequently washed with PBS. Secondary antibodies were from Cappel (West Chester, PA), and included FITC-conjugated affinity purified goat anti–human IgG, anti–mouse IgG, and anti–mouse IgM, and anti–rabbit IgG antibodies; Rhodamine goat anti–rabbit IgG antibodies; and Texas Red sheep anti–mouse IgG antibodies. All secondary antibodies were applied at 2.5 μg/ml. F-actin was detected by 30 min incubation at 37°C with 1.7 μg/ml FITC-phalloidin. Counterstain with propidium iodide (0.2 μg/ml) was for 5 min in PBS.

For immunolocalization of cyclin B, cells were fixed 5 min in methanol at −20°C, washed with PBS, and then incubated with primary and secondary antibodies, as above. For immunodetection of Eg5, cells were rinsed in 45 mM Pipes, 45 mM Hepes, 10 mM EGTA, 5mM $MgCl_2$, pH 6.9 [PHEM, Bailly et al., 1989]. Cells were then permeabilized with PHEM + 0.1% Triton X-100 for 40 s, and were then fixed 6 min in methanol at −20°C.

The following antibodies were utilized for indirect immunofluorescence microscopy. JH human autoimmune serum (Andreassen et al., 1991), a kind gift of M. Wener (University of Washington, Seattle) was used at a 500-fold dilution to detect TD-60. CHO1 ascites fluid (Sellitto and Kuriyama, 1988), a kind gift from R. Kuriyama (University of Minnesota, Minneapolis), was used at a 1,000-fold dilution to detect MKLP-1. Rabbit polyclonal antiserum 1.6 specific for CENP-E (Yen et al., 1992), obtained from T. Yen (Fox Chase Cancer Research Center, Philadelphia), was used at a 200-fold dilution. Anti-β-tubulin ascites antibody from Sigma (TUB 2.1) was used at a 400-fold dilution. L3, an antibody specific for non-tyrosinated tubulin (Paturle-Lafanechère et al., 1994), was obtained from L. Paturle-Lafanechère and D. Job (DBMS, CENG, Grenoble, France), and was used at a 250-fold dilution to detect centrosomes in mitotic cells. Anti-lamin B human autoimmune serum (patient F) and rabbit anti-lamin B antiserum (Chaudhary and Courvalin, 1993), gifts from J.-C. Courvalin (Institut Jacques Monod, Paris), were used at dilutions of 400- and 150-fold, respectively. MPM-2 mouse monoclonal antibody (Davis et al., 1983), supplied by J. Kuang (M.D. Anderson Cancer Center, Houston), was used at a 750-fold dilution of the ascites fluid. GNS-1 hybridoma supernatant, a gift from S. Schiff and E. Harlow (Massachusetts General Hospital, Boston, MA), was used at a 50-fold dilution to detect cyclin B1. Rabbit antiserum recognizing Eg5, a gift from M. Kress (CNRS, Villejuif, France), was used at a 50-fold dilution.

Images were registered with a MRC-600 Laser Scanning Confocal Apparatus (BioRad Microscience Division, Herts, England) coupled with a Nikon Optiphot microscope. Photographs were taken on TMAX-100 film (Kodak, Rochester, NY) with a Polaroid CI-3000 film recorder (Cambridge, MA). Color pictures were generated with a Sony UP-3000P Color Video Printer.

Quantitation of cells by microscopy was performed by selecting random fields and counting at least three sets of 250 cells for each time point and condition.

Determination of Mitotic Index

The mitotic index after treatment with nocodazole was determined (Fig. 1) using either a two-dimensional flow cytometric analysis with MPM-2 antibody and propidium iodide (Andreasssen and Margolis, 1994), or by chromosome condensation, as detected microscopically by staining with

1. *Abbreviations used in this paper*: DCB, dihydrocytochalasin B; MKLP-1, mitotic kinesin-like protein-1.

propidium iodide (Figs. 3 and 9). For flow cytometric analysis, data were collected using a Becton-Dickinson FacScan, and the mitotic region was quantitated using Lysys II software.

Results

Members of the cytochalasin family of compounds, including DCB, cause mammalian cells to fail in cell cleavage (Carter, 1967; Atlas and Lin, 1978; Aubin et al., 1981). At 10 μM DCB, the vast majority of HeLa cells completely fail in both furrow formation and in cleavage (Fig. 1 *A*).

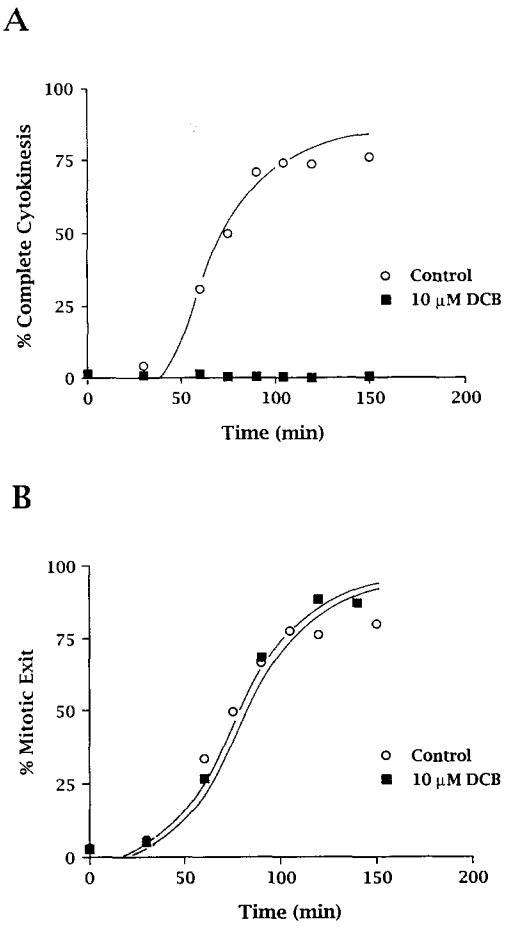

Figure 1. Cell cleavage and mitotic exit after nocodazole release. (*A*) HeLa cells, released at time 0 from nocodazole arrest, begin cytokinesis by 60 min, and have largely completed cleavage by 90 min, whereas cells treated with 10 μM DCB at the time of nocodazole release exhibit no cleavage. Coverslips were removed from culture at the timepoints indicated, and cells were prepared for immunofluorescence microscopy with anti–TD-60 antiserum and anti-lamin B antibody. Cleaved cells, identified by the presence of a midbody (TD-60 antigen) bridging between two interphase cells, were scored as a percent of the initial mitotic population. (*B*) Failure of cleavage does not impede mitotic exit. Cells were treated with DCB and time points taken as in *A*, and labeled with anti-lamin B antibody and anti–TD-60 antiserum. Control cells were scored positive for mitotic exit by the presence of interphase nuclei and a midbody; DCB-treated cells were scored positive if they contained two nuclei with lamin borders. All data were recorded as a percentage of the mitotic cells present at time 0. Each time point represents at least three counts of 300 cells each.

Control cells, released from a 12-h block in 0.04 μg/ml nocodazole, progress with reasonable synchrony through mitosis, and complete cytokinesis with a $t_{1/2}$ of ~70 min. In contrast, very few cells (<0.4% of mitotic cells) that have been given DCB at the time of release from nocodazole block give evidence of initiating cleavage through the entire course of the experiment.

The concentration of DCB used was determined in preliminary experiments, in which a range of DCB concentrations were tested for their ability to suppress furrow formation and cell cleavage. In accord with our previous report (Andreassen et al., 1991) there was a dose-dependent effect of DCB upon furrowing. Complete furrow formation occurred at 2 μM DCB, followed by subsequent reversion and formation of binucleate cells. DCB at 5 μM moderately suppressed furrowing, and doses of 10 μM or higher were completely effective. At high concentrations, no more than 0.4% of mitotic cells display evidence of any furrowing. We had previously reported that cleavage could occur at high DCB concentrations (Andreassen et al., 1991), but this occurs with very low frequency.

Failure to undergo cleavage does not substantially impede mitotic exit. By the criterion of reformation of a nuclear lamin border, both control and DCB-treated cells exit mitosis with approximately the same kinetics (Fig. 1 *B*). At the time of reformation of a nuclear envelope (see Fig. 2, *D* and *E*), these cells are also in interphase by the criteria of the decondensation of chromatin and the reformation of nucleoli.

Lamin B is a highly discriminant marker that distinguishes between interphase or mitotic states (Chaudhary and Courvalin, 1993). Interphase cells display a brightly staining lamin B ring around their nuclei (Fig. 2 *A*) and show little cytoplasmic background. In contrast, lamin is dispersed from chromatin upon nuclear disassembly, and remains dispersed both at metaphase (Fig. 2 *B*), and as cells proceed through cleavage at the end of mitosis (Fig. 2 *C*). Cytoplasmic accumulations of lamin are normally apparent in all mitotic cells. In accord with previous observations (Chaudhary and Courvalin, 1993), we find that reformation of lamin borders normally occurs after the completion of furrowing. By the criterion of lamin label, DCB-treated cells have reformed nuclei by 90 min after nocodazole release and reenter interphase without cleavage (Fig. 2 *D*).

Curiously, although there is a nearly complete lamin border around the nuclei, there is frequently a small region facing the opposing nucleus that is devoid of lamin. A field of DCB-treated cells with reestablished lamin borders is shown in Fig. 2 *E*.

In Fig. 2 and in subsequent figures, a "postmitotic" cell denotes an uncleaved cell in a transient state in which the nuclei have reconstituted an interphase character (Fig. 2, *D* and *E*), while mitotic elements such as a mitotic spindle and a telophase disc are retained (see Fig. 6).

Retention of the Telophase Disc in Uncleaved Cells

Because of the potential role of the telophase disc in cytokinesis, we have examined its behavior in DCB-treated cells (Fig. 3). When HeLa cells are recovered into 10 μM DCB, the telophase disc is formed at the appropriate time,

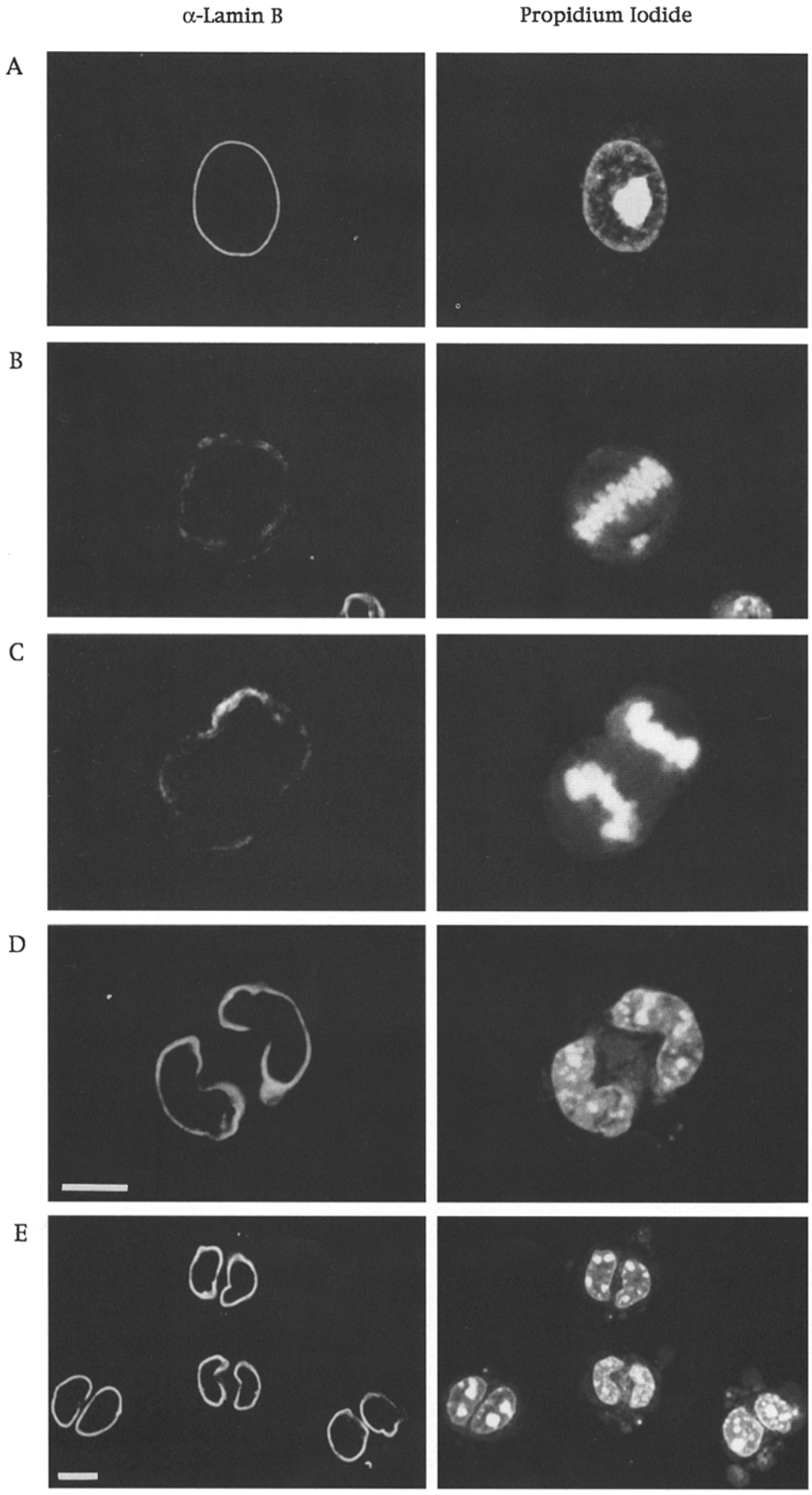

Figure 2. Reformation of nuclei in cleavage arrested cells. HeLa cells, synchronized in mitosis by release from nocodazole arrest, were analyzed by immunofluorescence microscopy with anti-lamin B antibodies (*left*) and DNA stain (*Propidium Iodide*, *right*). (*A*) Control interphase. A control interphase cell, showing a lamin border around an intact nucleus containing a nucleolus that is highly stained by propidium iodide. (*B*) Control metaphase. A control metaphase cell, showing aligned chromosomes and dispersed lamin. (*C*) Control telophase. A control telophase cell, with dispersed lamin. (*D*) Postmitotic DCB-treated cell. DCB-treated cell in blocked cleavage at 90 min after nocodazole release. A reestablished lamin rim has almost completely encircled the chromatin. Note the indentations and gaps in lamin borders where the nuclei face each other. Propidium iodide stain (*right*) shows reconstituted nuclei with nucleoli evident. (*E*) Postmitotic DCB-treated cell field. A field of DCB-treated cells in blocked cleavage, showing reconstituted nuclei with lamin borders. Anti-lamin primary antibodies were detected with FITC-goat anti-rabbit IgG antibodies. Bars, 10 μm.

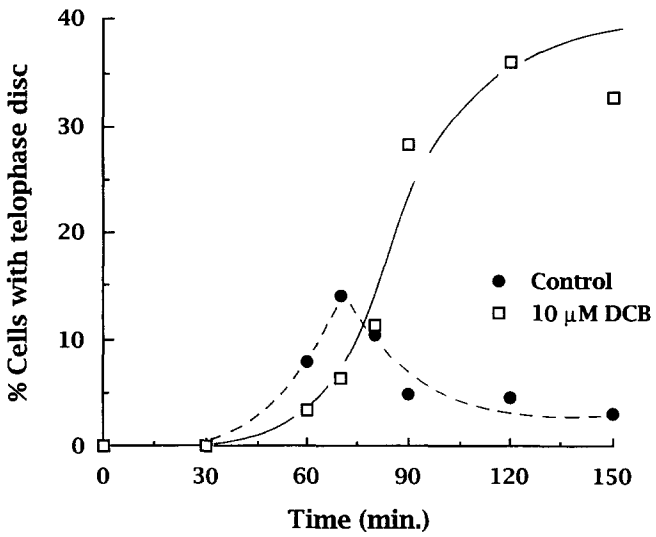

Figure 3. Retention of the telophase disc in the presence of DCB. Synchronous control cells, released from nocodazole-induced mitotic arrest, display a telophase disc for a brief period of time during late mitosis. In contrast, cells released into 10 μM DCB form the telophase disc at approximately the same time, but retain it for a prolonged period of time compared to controls. Cells were fixed on coverslips at timepoints and prepared for immunofluorescence microscopy. A telophase disc is defined by the linear arrangement of TD-60 antigen present at the equatorial position between two separated sets of chromatin (see Fig. 4). Each data point represents at least three counts of 500 cells each. Data are expressed as a percent of the initial mitotic index. The mitotic index was determined at 0, 30, and 60 min after nocodazole release by calculating the ratio of cells with condensed chromosomes relative to total cells.

but then persists for a prolonged period of time in the absence of cleavage (Fig. 3). In contrast, the telophase disc is present only transiently during cleavage in a control population released from nocodazole synchronization.

The telophase disc, as visualized with the TD-60 marker (Andreassen et al., 1991), is present at the equatorial position of control cells in early cleavage (Fig. 4 *A*), and remains at the precise position of cleavage through the entire cleavage process (Fig. 4 *B*). Similarly, in the presence of 10 μM DCB, the telophase disc is evident at the equatorial position between the two daughter sets of chromatin (Fig. 4 *C*). Notice that, unlike cleaving control cells where chromosomes are evident until cleavage has completed (Fig. 4 *B*), DCB-blocked cells often contain reconstituted interphase nuclei simultaneously with a telophase disc (Fig. 4, *C* and *D*). Additionally, in the reconstituted interphase nuclei shown in Fig. 4 *C*, nucleoli are evident.

TD-60 is one of a family of proteins that accumulate at the position of the telophase disc in late anaphase and telophase (Andreassen et al., 1991; Earnshaw and Bernat, 1991). Two such proteins, CENP-E (Yen et al., 1992) and MKLP-1 (Nislow et al., 1992), have microtubule motor domains. In DCB-treated cells, both CENP-E and MKLP-1 persist at the position of the telophase disc after interphase nuclei have been reconstituted (Fig. 4, *E* and *F*).

We previously presented evidence that the telophase disc is an integral structure independent of the mitotic spindle (Andreassen et al., 1991). This conclusion was based on the fact that TD-60, when incorporated into the telophase disc, resists cold temperature treatment, which causes the complete disassembly of the anaphase spindle in HeLa cells. Further evidence that TD-60 distributes independently of the anaphase spindle is presented in Fig. 5. For this analysis, TD-60 distribution is compared with that of CENP-E and MKLP-1 in late anaphase cells. CENP-E and MKLP-1 are microtubule associated proteins that distribute to the equator of the anaphase spindle (Sellitto and Kuriyama, 1988; Yen et al., 1991). The comparison clearly shows that TD-60 is associated with the cortex beyond the central mitotic spindle. As shown by color merge of double-label images for TD-60 and MKLP-1, these antigens are colocalized in the region of overlap of interpolar microtubules in the center of the cell (Fig. 5 *A*). TD-60, but not MKLP-1, extends across the equator of the cell to the cortex. A plot of pixel intensity for both TD-60 and MKLP-1, as scanned across the equator of the cell, demonstrates that TD-60 alone traverses the cell to the cortex. Similar results, demonstrating colocalization of TD-60 and CENP-E in the region of spindle overlap, but not at the cortex are also shown (Fig. 5 *B*).

Retention of the Mitotic Spindle in Uncleaved Cells

TD-60 and other mitotic antigens migrate to the equatorial position between the chromosome sets during late mitosis through an association with the mitotic spindle (Andreassen et al., 1991; Earnshaw and Bernat, 1991). On this basis, we have proposed that the mitotic spindle templates the formation of the telophase disc (Margolis and Andreassen, 1993). Given that the telophase disc persists in the absence of cleavage, we asked if microtubule elements of the mitotic spindle might also be present.

In a synchronous population of cells that has been blocked in cleavage by 10 μM DCB, one indeed frequently finds a persistent spindle lying between two reconstituted nuclei, containing a telophase disc at its equator, as shown in Fig. 6 *A*. By phase contrast, it is clear that each cell is uncleaved and contains two reconstituted nuclei, while the anti-tubulin signal reveals a persistent spindle composed of microtubules lying between the two nuclei.

Additional evidence that interphase nuclei coexist with a mitotic spindle comes from double label staining with lamin B and anti-tubulin antibodies (Fig. 6 *B*). With these two labels, it is evident that nuclei with lamin borders are present in the same cell as an apparent mitotic spindle. The persistent spindle is focused at its poles, in contrast with the normal parallel array of microtubules present in the spindle in telophase. We designate the persistent spindle, which is present in cells that have failed in cleavage and have reconstituted interphase nuclei, as a "postmitotic" spindle. Frequently, as seen here, the nuclei deform around the ends of the spindle. Interestingly, at the point of juncture between the spindle and the nuclei, one often finds a hole in the lamin border (see Fig. 2), suggesting that the persistent spindle prevents lamin deposition where it contacts the chromatin.

The mechanism by which the morphology of the postmitotic spindle is retained is not clear. Normally, the mitotic spindle has two focal origins, the two spindle poles, where the microtubules converge on the centrosomes. As the

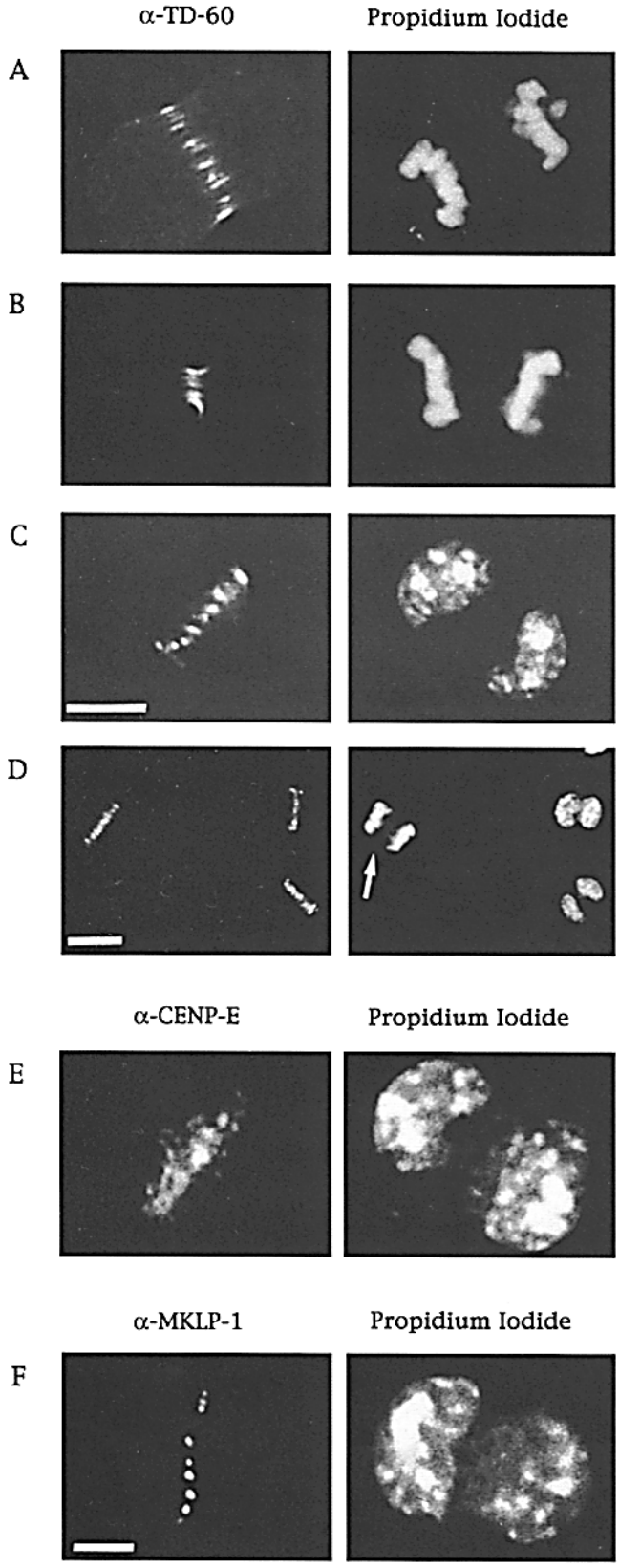

Figure 4. Persistence of the telophase disc in cleavage-arrested cells. (*A*) Control cell, mid-telophase. The telophase disc, marked with antibodies to TD-60, normally is present at the equatorial position between chromosomes of late anaphase cells and early telophase cells, as shown here. Chromosomes are shown at right, counterstained with propidium iodide. (*B*) Control cell, late telophase. The telophase disc remains in the precise position of cleavage during telophase. (*C*) Postmitotic DCB-treated cell. In a DCB-blocked postmitotic cell, containing reconstituted nuclei, the telophase disc is retained at a position midway between the nuclei. (*D*) Postmitotic DCB-treated cell field. A field of cells blocked in 10 μM DCB, including two postmitotic cells and a mitotic cell in late anaphase (*arrow*), demonstrates that the telophase disc undergoes no apparent change during transition of the cell to the postmitotic state. (*E* and *F*) Postmitotic DCB-treated cells. (*E*) CENP-E and (*F*) MKLP-1, two microtubule motor proteins, also are retained at the position of the telophase disc in DCB blocked postmitotic cells. Bars: (*C*) 10 μm; (*D*) 20 μm; (*F*) 5 μm.

centrosomes normally are present on the exterior surfaces of the chromosome sets during anaphase and telophase, we asked where they were relative to the postmitotic spindles. Using an anti-glu-tubulin marker, demonstrated to be specific for mitotic centrosomes (Paturle-Lafanechère et al., 1994), we find that centrosomes in DCB-treated cells are distinctly separate from the poles of the postmitotic spindle. This is in contrast with controls, where the centrosomes are always present at the spindle poles (Fig. 7). In both cases, the centrosomes are present on the exterior surfaces of the chromatin.

It is evident that the DCB-blocked cell retains mitotic character with respect to its spindle after the point in time when the cell's chromatin has reentered interphase. With respect to several standard mitotic markers, the cell has reentered interphase, although it retains a telophase disc. Cyclin B is normally degraded at the onset of anaphase (Whitfield et al., 1990; Pines and Hunter, 1991). DCB-treated cells that have progressed past anaphase and have reformed nuclei are therefore negative for cyclin B, as expected (Fig. 8 *A*). For comparison, a prophase cell in the same field is strongly positive for cyclin B. Control cells, released from nocodazole arrest, similarly display a cyclin B signal only until the onset of anaphase (data not shown).

MPM-2 antibodies detect mitosis-specific phosphoepitopes (Davis et al., 1983). Postmitotic cells treated with DCB (Fig. 8 *B*) display very little MPM-2 reactivity, whereas cells at prophase and metaphase display clear signals. By comparison to DCB-treated cells, control cells in mid-cleavage are still moderately positive for MPM-2, and in particular display centrosomal signals (Fig. 8 *C*, *arrow*).

The postmitotic spindle retains some mitotic character. This is evident from the continued presence of the mitosis specific proteins CENP-E and MKLP-1 (Fig. 4) at the spindle equator. We also assayed for the presence of another motor protein, Eg-5, that has been reported present only on microtubules in the mitotic spindle (Sawin et al., 1992), and absent from interphase microtubules. Eg-5 is present on postmitotic spindles, with an abundance that appears equivalent to its presence on a control metaphase spindle (Fig. 8 *D*). The signal then disappears as the postmitotic spindle degenerates (data not shown).

Synchronous Cleavage of Postmitotic Cells

The continued presence of the mitotic spindle and the telophase disc in interphase cells that have failed in cleavage suggests that these structures may play a role in the cleavage mechanism and are normally disassembled in the

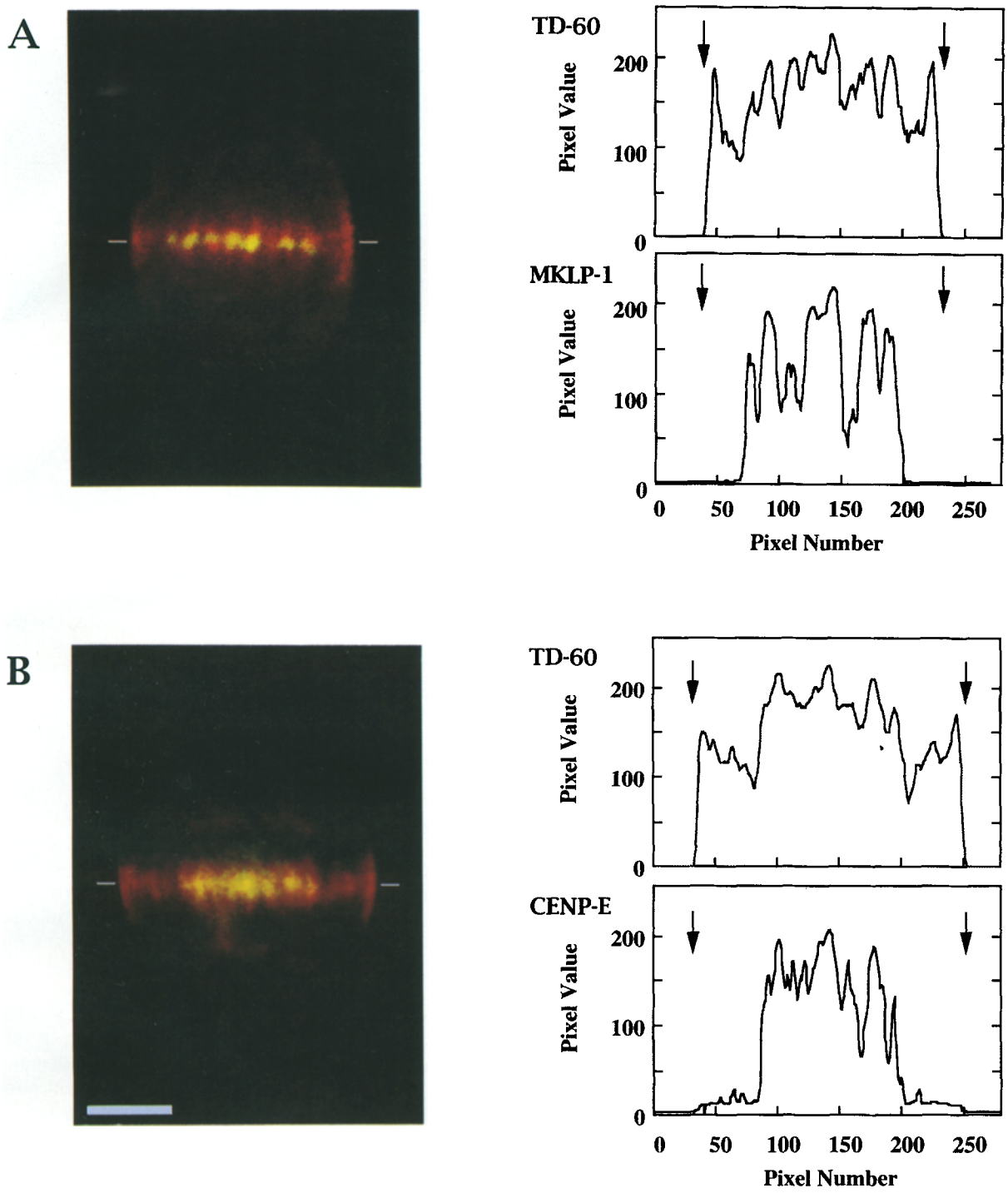

Figure 5. TD-60 is present throughout the equator of late-anaphase cells. (*A*) TD-60 (*red*) and MKLP-1 (*green*) partially codistribute at the spindle equator during late anaphase, as shown here with a color merge of a double-label image collected as an optical section by confocal microscopy (*left*). TD-60 consistently extends beyond the MKLP-1 signal toward the cell cortex, as shown here. The image is yellow where TD-60 and MKLP-1 coincide, and is red where TD-60 alone is distributed. Scans of pixel intensity across the equator (the axis of the scan indicated by lines on the photo at left) are displayed for TD-60 and MKLP-1 at right. (*B*) A color merged image of TD-60 (*red*) and CENP-E (*green*) in a late anaphase cell is shown at left. Scans of pixel intensity for TD-60 and CENP-E are shown at right. Arrows indicate the position of the cell cortex. Bar, 10 μm.

course of successful cleavage. The potential importance of the mitotic spindle and the telophase disc was tested by the ability of the postmitotic cell to resume cleavage upon the removal of DCB.

A synchronous population of postmitotic cells, suppressed in cleavage by the presence of DCB, will cleave within minutes of the removal of DCB. In this experiment, DCB was removed from the medium at 90 minutes after mitotic recovery from nocodazole arrest (Fig. 9 *A*). For the purpose of this analysis, postmitotic cells were distin-

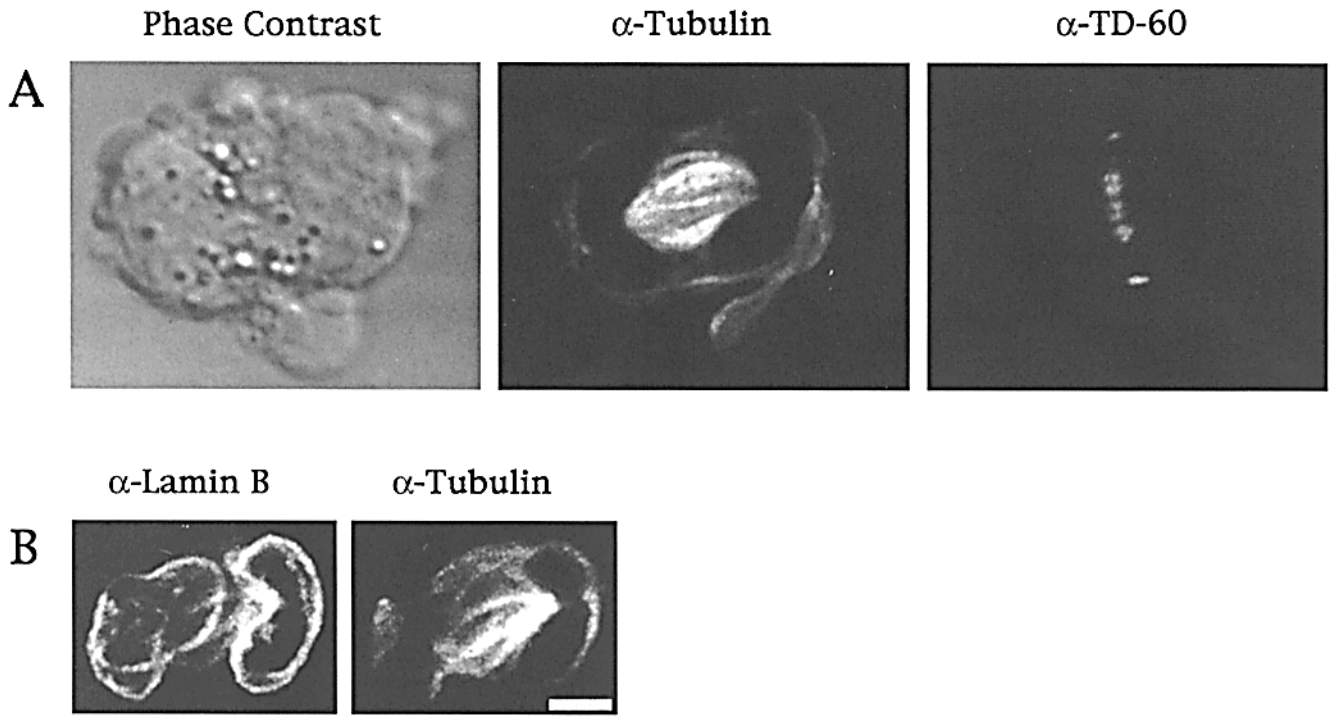

Figure 6. A mitotic spindle and nuclei with lamin borders can coexist in DCB-treated cells after inhibition of cleavage. (*A*) An uncleaved cell in the presence of DCB has exited mitosis by the criterion of intact nuclei visible by phase contrast microscopy (*left*); but contains a mitotic spindle structure (*middle*) between the nuclei and a telophase disc (*right*) detected by TD-60 immunofluorescence. This cell was imaged on a confocal microscope after preparation with mouse anti-tubulin antibody and with human anti–TD-60 antiserum. Note the extensive blebbing of the cell visible by phase contrast microscopy. (*B*) Another postmitotic cell treated with DCB shows the presence of interphase lamin borders around nuclei (*left*). The same cell also contains an apparent mitotic spindle (*right*), detected with antibodies specific for tubulin. Bar, 5 μm.

guished by the presence of two nuclei and of a telophase disc spanning the equator between the two nuclei. Cells in the process of cleavage appear within minutes of the removal of DCB from the culture medium, and reach a peak at approximately 10–15 min after drug washout, and a population of cells that have completed cleavage accumulates shortly thereafter (Fig. 9 *A*, *open triangles*).

The capacity to resume cleavage upon removal of DCB diminishes with time after recovery from nocodazole arrest, and is strongly correlated with the continued presence of the postmitotic spindle and the telophase disc (Fig. 9 *B*). Beginning at 90 min after recovery from nocodazole arrest, binucleate cells, in which the telophase disc and the postmitotic spindle have degenerated, progressively accumulate. At later times, as the population of cells containing a postmitotic spindle and telophase disc declines, the capacity to cleave after removal of DCB strongly diminishes. A comparison of the time of mitotic exit in DCB (Fig. 1 *B*) with the time of loss of cleavage competence (Fig. 9 *B*) indicates that, on average, postmitotic cells remain cleavage competent for approximately one hour after mitotic exit.

The synchrony of cell cleavage after removal of DCB is clearly evident in microscopic fields. Before DCB removal, fields of postmitotic cells containing both spindles and reformed interphase nuclei are evident (Fig. 9 *C*, *left*), but by 15 min after DCB washout, cleavage is widespread among this population (Fig. 9 *C*, *right*). After release from DCB, cleaving cells characteristically contain equatorially compacted spindles. Cleaved cells with interphase nuclei, as visualized by phase contrast microscopy, contain a compacted telophase disc at the site of cleavage (Fig. 9 *D*). By contrast, in the continued presence of DCB, degeneration of both the postmitotic spindle and the telophase disc progresses steadily in postmitotic cells, finally yielding binucleate G_1 cells.

The potent capacity of DCB to block cleavage is of course a direct consequence of the requirement for F-actin in the cleavage process. The specific role of actin in the cleavage process in mammalian cells is, however, not completely clear. During normal cleavage, only a small percentage of mammalian cells exhibit a clear concentration of actin at the furrow (Cao and Wang, 1990). Frequently, the actin that accumulates in an array parallel with the cleavage axis is evident only on the cell surface in contact with the substratum (Fishkind and Wang, 1993). We (Andreassen et al., 1991) and others (Krishan, 1972; Sanger and Holtzer, 1972) have shown that lower concentrations of cytochalasins (e.g., 2 μM DCB) cause extensive disassembly of actin but do not impede furrowing.

We have therefore examined the state of actin assembly during DCB blockage and recovery in HeLa cells, using fluorescent phalloidin, a probe that is specific for assembled actin (Wulf et al., 1979). Typically, in accord with previous reports (Cao and Wang, 1990; Fishkind and Wang, 1993), we find little evidence for specific accumulation of actin at the cleavage furrow during control HeLa cell cleavage (Fig. 10 *A*). Instead, typically, F-actin is uni-

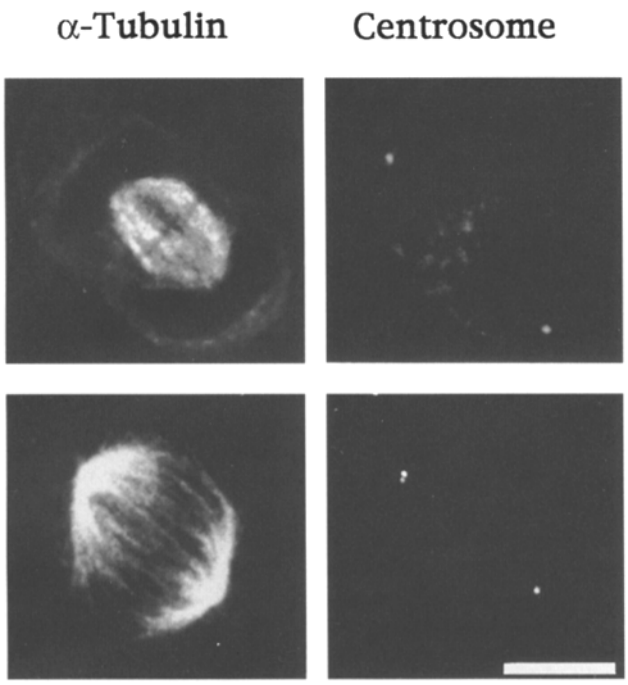

Figure 7. (*Top*) Postmitotic DCB-treated cell. Postmitotic spindles are not associated with centrosomes. In postmitotic DCB-treated cells, where nuclei and a spindle coexist, the centrosomes (*top right*) are always present on the outer sides of the nuclei, opposite to the position of the spindle poles (*top left*). (*Bottom*). This is in comparison to a normal metaphase spindle (*bottom left*), in which the centrosomes (*bottom right*) are localized to the spindle poles. Note also that the postmitotic spindle is substantially smaller than a control metaphase spindle, and has a dark equatorial bar that corresponds to the telophase disc. Centrosomes were visualized with anti–glu-tubulin, which is specific for centrosomes in mitotic cells (Paturle-Lafanechère et al., 1994). Centrosome position relative to the mitotic spindle was verified by overlay of digital images collected with a confocal microscope. Bar, 10 μm.

formly dispersed throughout the cell cortex. In the presence of 10 μM DCB, actin is randomly associated with the cell cortex, with the exception of local accumulations in the surface blebs that are characteristic of DCB treatment (Fig. 10 *B*). Thus the disruption of cytokinesis by 10 μM DCB is correlated with the disruption of cortical actin organization. In contrast, during synchronous cleavage of postmitotic cells after 10 min of recovery from DCB treatment, we find actin has specifically reassociated with the cell cortex at the position of the cleavage furrow (Fig. 10, *C* and *D*). Cells in which the telophase disc contacts only one cortical surface undergo a one-sided cleavage after release from DCB treatment (Fig. 10 *E*). One can see the association of the telophase disc and actin at the furrowing side during one-sided cleavage. This may suggest that the position of the telophase disc, or of the spindle, locally determines the position of furrow formation. Cells in which the telophase disc has degenerated or in which it makes no contact with the cell cortex (data not shown), consistently fail to cleave during DCB recovery. This fact argues against the contrary possibility, that furrowing causes the cortex to locally contact the telophase disc.

Discussion

We have presented evidence that cleavage failure induced in HeLa cells by DCB is accompanied by a transient "postmitotic" state. We define the cell as postmitotic when interphase nuclei have been reconstituted, but the mitotic spindle and telophase disc remain. The capacity for cell cleavage is preserved in these postmitotic cells, and a synchronous cell cleavage can be induced by removal of DCB. In postmitotic cells, the cleavage furrow forms only when and where the telophase disc makes contact with the cell cortex.

We draw several conclusions from these observations. First, the reconstitution of all elements of the interphase cell does not necessarily occur synchronously. Second, cytokinesis is dissociable from mitosis. Third, the anaphase spindle and telophase disc may act integrally in establishing the time and place of furrow formation in mammalian cells. Finally, cleavage can be induced to occur with high synchrony in cells recovering from DCB. With the methods described here, it should now be possible to produce a synchronous model system for the analysis of mammalian cell cleavage independent of concurrent mitotic events.

Postmitotic Cells: Interphase or Mitotic?

We have demonstrated that, in the event of failure of cell cleavage, the mitotic spindle and the telophase disc are retained into interphase. Interphase is here defined by the disappearance of mitosis specific markers such as MPM-2 and cyclin B, and by the reconstitution of interphase nuclei. The nuclei in these cells are recognized as interphase on the basis of several characteristics, including a reformed lamin border, decondensed chromatin and the presence of nucleoli.

DCB-treated cells retain this partial and selective mitotic character for a period of time in G_1, after which the spindle and telophase disc degenerate. The various mitosis-specific elements arise at the onset of mitosis under the control of the protein kinase $p34^{cdc2}$ (Lamb et al., 1990; Nigg, 1991). Despite the fact that $p34^{cdc2}$-cyclin B kinase activity is rapidly degraded at the onset of anaphase (Hunt et al., 1992; Holloway et al., 1993), elements of the mitotic spindle in the anaphase cell are normally retained until cleavage is complete. The mechanism by which mitotic character is retained through the period of anaphase and telophase is unknown, but may involve late mitotic protein kinases that are active specifically at anaphase and telophase (Fenton and Glover, 1993; Toyn and Johnston, 1994).

Postmitotic cells in the presence of DCB possess a microtubule structure that appears to represent the remaining interpolar elements of the anaphase mitotic spindle. It perhaps shares some similarity with stembody microtubule bundles of telophase cells, as the residual spindle, like the stembody, lacks association with centrosomes. The centrosomes are present on the opposite side of the nuclei in postmitotic cells, leaving open the interesting question of the mechanism by which the integrity of the postmitotic spindle is maintained.

In addition to retention of the form of a mitotic spindle, the postmitotic spindle retains association with the mitosis specific (Sawin et al., 1992) microtubule motor protein Eg-5.

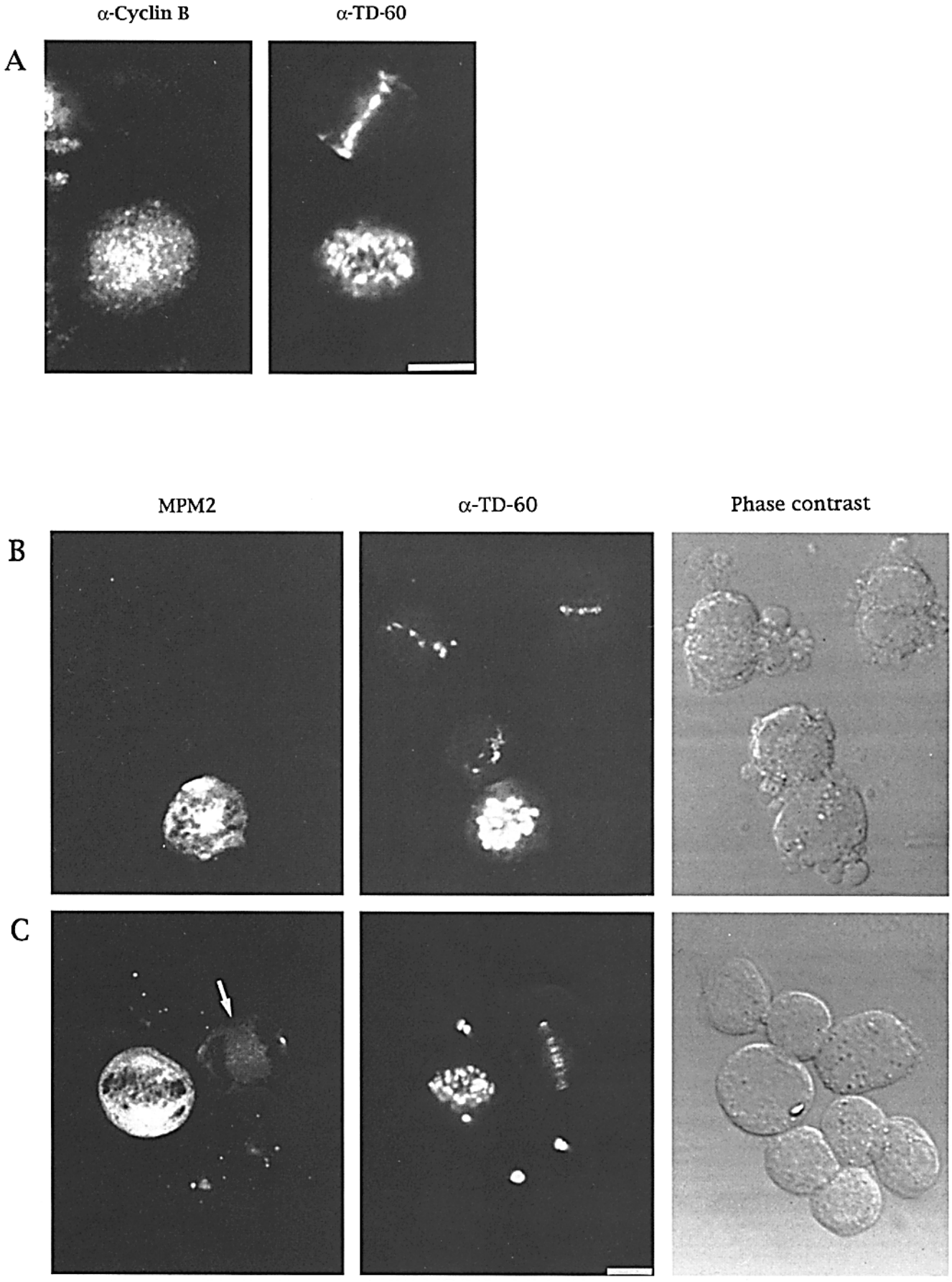
α-Cyclin B
α-TD-60
A
MPM2
α-TD-60
Phase contrast
B
C

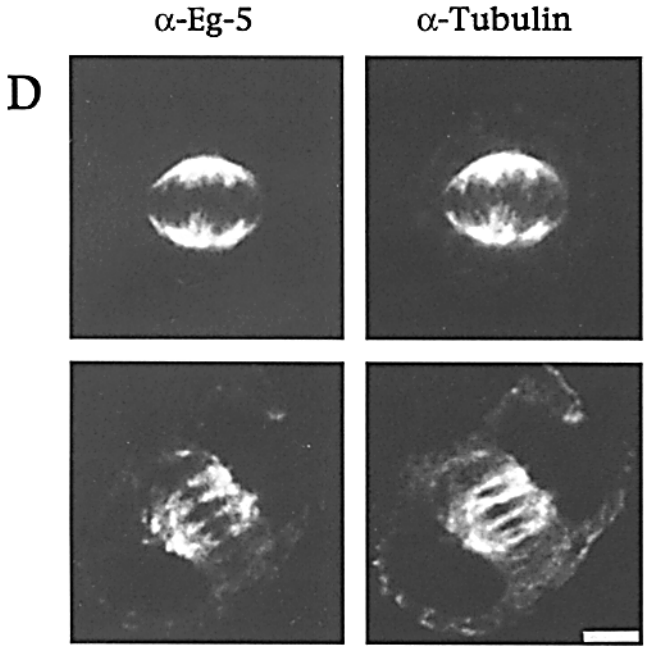

Additionally, at its equator we have found several mitosis specific antigens that normally migrate toward the equatorial position of the spindle during anaphase, including TD-60, CENP-E, and MKLP-1. Such equatorial antigens may serve to maintain the anti-parallel microtubules of the two half spindles in register at their overlapping ends (Nislow et al., 1990), and thus may be responsible for the spindle shape of the microtubule array in postmitotic cells. The spindle poles might perhaps represent parallel microtubules associated by cross-linking at their minus ends.

In addition to a postmitotic spindle, DCB-treated postmitotic cells also retain a telophase disc. Although the telophase disc can exist independently of microtubules (Andreassen et al., 1991), it seems that the postmitotic spindle and the telophase disc interact as an integral element in postmitotic cells. The telophase disc is present perpendicularly at the center of the postmitotic spindle. At longer times after reentry into G_1, both the postmitotic spindle and telophase disc degenerate. Retention of both the microtubule spindle and the telophase disc in postmitotic cells may be important to the capacity of the cell to resume cleavage upon removal of DCB (see below).

Independence of Cytokinesis from Mitosis

Cells that retain a spindle and a telophase disc, but which are otherwise interphase in character, cleave after release from treatment with DCB. This demonstrates that cytokinesis can occur independently from normally concurrent events in mitosis. Since cyclin B has been degraded in postmitotic cells that can cleave upon removal of DCB, it is apparent that cytokinesis does not require the presence of active $p34^{cdc2}$. Perhaps specific late mitotic kinases, such as polo (Fenton and Glover, 1993) are involved in the regulation of cytokinesis.

In comparison to other events in the cell cycle such as S-phase and the onset of mitosis, the molecular control of mammalian cell cleavage has not been substantially elucidated. An important impediment to molecular analysis of mammalian cell cleavage has been the lack of a synchronous in vitro model system with which to study this process.

The system we describe here of postmitotic mammalian cells undergoing synchronous cleavage upon recovery from DCB lends itself to the development of a model system for the in vitro study of mammalian cell cleavage mechanisms. This system would offer the potential of investigating cell cleavage independent of mitosis. The only component apparently lacking in the DCB-blocked cell is sufficient assembly competent actin to complete cleavage. We hope to be able to reconstitute synchronous cleavage by addition of assembly competent actin in an open cell system. Such a system promises to permit the analysis of the control of cytokinesis, and of the role of the telophase disc, the residual mitotic spindle and the cortical ring of actin in cleavage.

The Role of the Telophase Disc and of Actin in Cleavage

Our experiments have demonstrated conclusively that organized actin is essential to the furrowing process during mammalian cell cleavage. There have been conflicting reports concerning whether cytochalasins actually prevent furrow completion (reviewed in Margolis and Andreassen, 1993). In accord with others, we have previously demonstrated that a concentration of DCB sufficient to depolymerize interphase F-actin (2 μM) does not impede furrowing of HeLa cells (Krishan, 1972; Sanger and Holtzer, 1972; Andreassen et al., 1991). The cleavage furrows separating the daughter cells finally revert during early interphase, giving rise to binucleate cells. Here we show that a

Figure 8. Assay for mitotic markers in DCB-treated postmitotic cells. (*A*) Confocal microscopic images of HeLa cells released from nocodazole block in the presence of DCB. By TD-60 signal, the cell at the bottom is in prophase, and contains abundant cyclin B (*left*). In contrast, the postmitotic cell, identified by a telophase disc (*right*), is negative for cyclin B. (*B*) Postmitotic DCB-treated cells. MPM-2 antigen is absent from the three postmitotic cells (*left*), while it is strongly positive in the prophase cell at bottom. The postmitotic cells are identified by the presence of telophase discs, detected with anti–TD-60 antibodies (*middle*). The two upper cells have nuclei, apparent in phase contrast (*right*). The third postmitotic cell has a degenerated telophase disc. (*C*) Control cells. In contrast, a control cell at the beginning of telophase has a faint residual stain for MPM-2 (*left, arrow*). For comparison, a pro-metaphase cell in the same field (*left, cell on left*) labels intensely with MPM-2 antibody; and three pairs of cells that have just exited mitosis, as determined by TD-60 antigen in midbodies (*middle*) and figure eight appearance (*right*), are not reactive with MPM-2 antibodies (*left*). (*D*) Control (*top*) and postmitotic DCB-treated cells (*bottom*). Eg-5, a microtubule motor protein that is specific for mitotic microtubules gives a signal (*top left*) that is coincident with that for tubulin in a metaphase control. In a DCB-treated cell, identified as postmitotic by the small central spindle and dark areas where there are reformed nuclei (*bottom right*), Eg-5 (*left*) is still coincident with the spindle microtubules (*right*). The same signal is obtained in experiments using Eg-5 antibody and propidium iodide counterstain. We have also observed that Eg-5 is absent from interphase microtubules in these cell populations (not shown). Bars (*A* and *C*) 10 μm; (*D*) 5 μm.

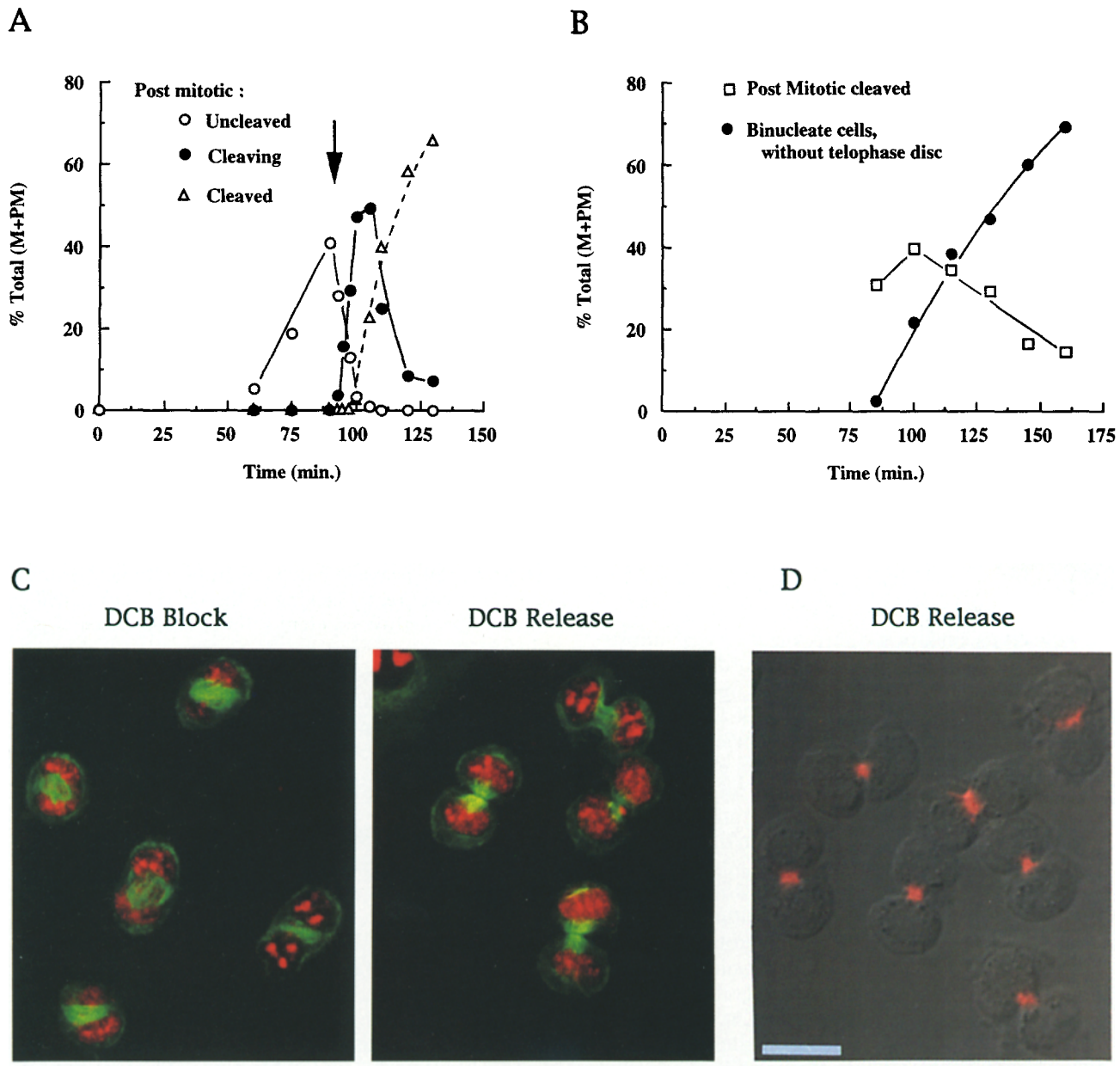

Figure 9. Rapid induction of synchronous cleavage in postmitotic cells upon release from DCB. (*A*) After removal of DCB, postmitotic cells initiate furrowing and progress to complete cleavage. HeLa cells were synchronized with nocodazole, released from nocodazole block into DCB (time 0), and finally released from the DCB block at 90 min (*arrow*), a time when a majority of cells have exited mitosis (see Fig. 1). Postmitotic cells in the process of cleavage (*solid circles*), were scored by the presence of TD-60 label at a constricting furrow lying between two nuclei. Cleaved cells (*open triangles*) were characterized by progression of the furrow to completion, and by the presence of a compacted TD-60 signal typical of cleaved cells (see *D*). Uncleaved postmitotic cells (*open circles*) were scored on the basis of the absence of detectable furrowing between the two nuclei. (*B*) The capacity for cleavage recovery correlates with the continued presence of the telophase disc and the postmitotic spindle. The ability to cleave was measured by release from DCB for 10 min after increasing intervals of DCB exposure. Time points indicate the point of fixation, representing the time of DCB release plus 10 min. Postmitotic cells were scored for their ability to form a complete cleavage furrow (*open squares*). At longer times, the population of postmitotic cells declined, and was replaced by binucleate G1 cells lacking a telophase disc and a postmitotic spindle (*closed circles*). In these experiments, the combined percentage of mitotic and postmitotic populations (*M + PM*)was determined at 90 min (*A*) or by the average of values from 60–90 min (*B*) after release from nocodazole. Cells with the phenotypes indicated are expressed as a percentage of the total mitotic and postmitotic cells (*M + PM*). Each point represents at least three counts of 250 cells each. (*C*) Merged confocal microscopic images of a field of HeLa cells either before cleavage after 105 min treatment with DCB (*left*), or with completed cleavage 15 min after release from 90 min treatment with DCB (*right*). Anti-tubulin label is imaged in green, and propidium iodide stain of chromatin is in red. (*D*) A merged confocal image of a field of cleaving cells 15 min after DCB release showing the phase contrast image in grey, and TD-60 in salmon red. Bar, 15 μm.

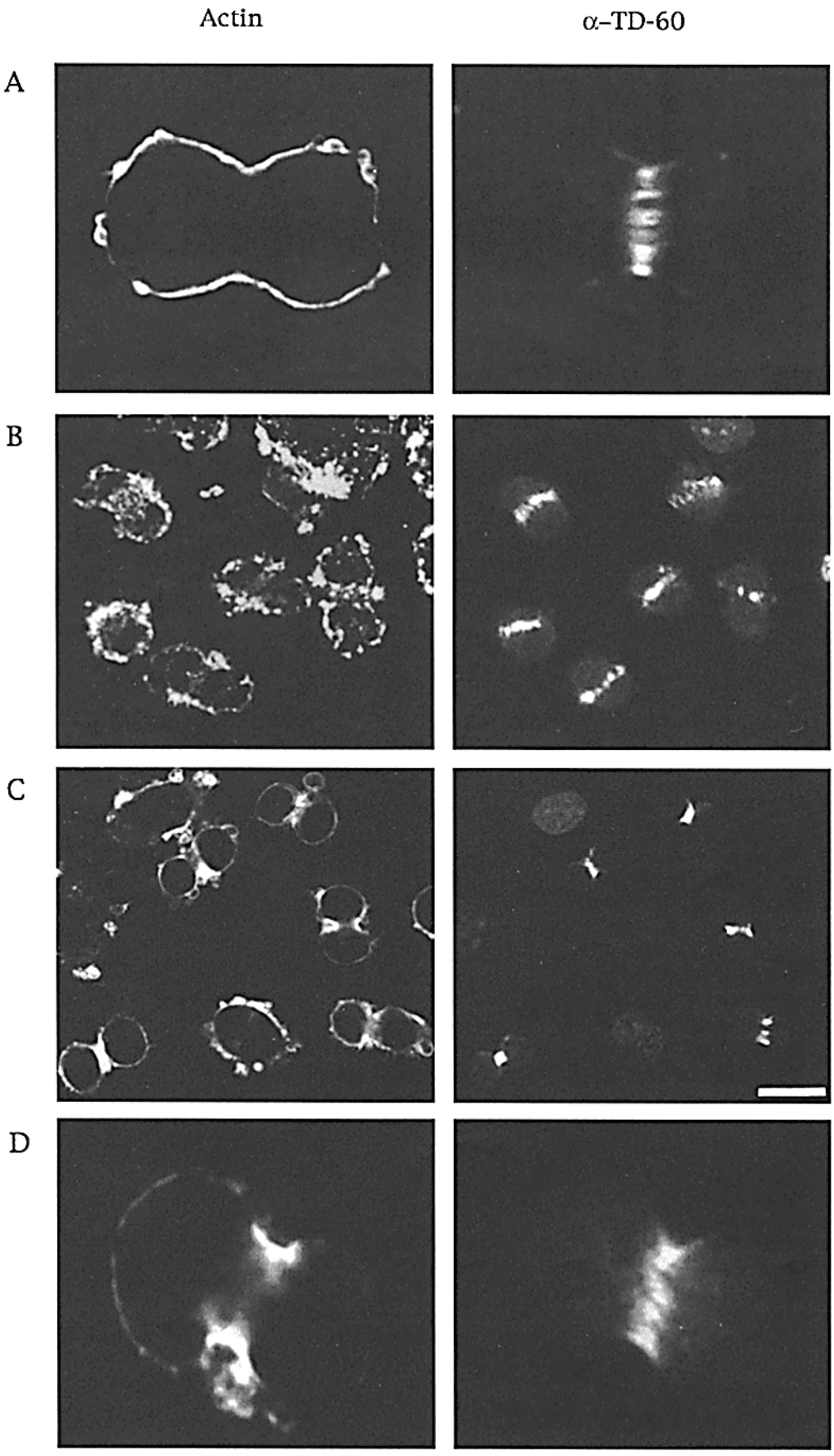

Figure 10. Distribution of actin in cleaving control and postmitotic cells. Polymeric actin, detected with FITC-phalloidin is shown at the left; the telophase disc marker TD-60 is at the right, except in (*E*), for which polymeric actin and TD-60 images are merged in color. (*A*) Control telophase cell. A control HeLa cell in mid-cleavage at 65 min after release from nocodazole arrest. Actin is dispersed randomly in the cell cortex, and exhibits no particular enrichment at the position of the furrow (TD-60 marker). This result is typical of the majority of cleaving cells. (*B*) In a field of cells in DCB block at 100 min after nocodazole release, actin is dispersed in random patches on the cell cortices. (*C*) At 10 min after release from DCB-induced cleavage block, the majority of cells in this field are in mid-cleavage and all cleaving cells show a marked concentration of actin polymer at the furrow. (*D*) Close-up of a cell in mid-cleavage, 10 min after release from DCB. (*E*) Close-up of two cells undergoing one-sided cleavage. The merged images show a coassociation of local concentrations of cortical actin, and telophase disc structures at the forming furrow during one sided cleavage after DCB release. Polymeric actin (*white*), detected with FITC-phalloidin, is highly concentrated at the site of the forming furrow and, internal to the actin, TD-60 antigen (*red*) gives evidence of cortically associated telophase disc elements. There is no concentrated cortical actin, nor TD-60, on the noncleaving side. Bars: (*A*, *D*, and *E*) 5 μm; (*B* and *C*) 20 μm.

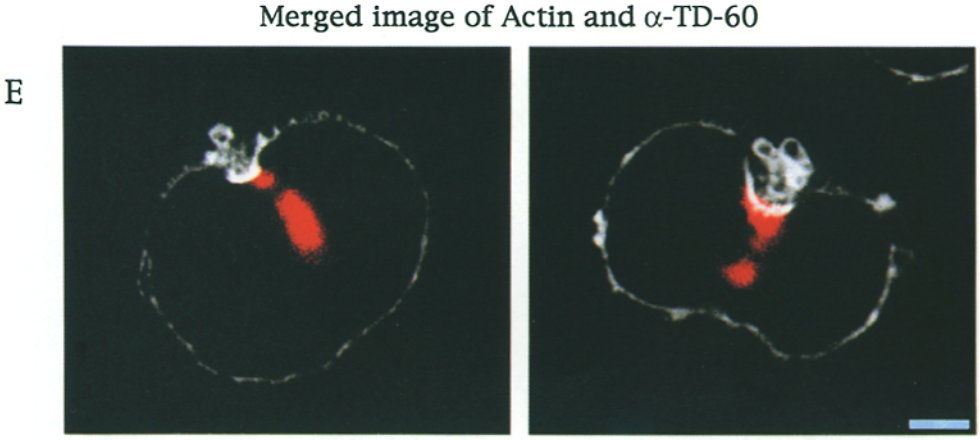

fivefold higher concentration of DCB, which disrupts the organization of cortical actin in mitotic cells, suppresses onset of furrowing in HeLa cells. Upon removal of DCB, cleavage in postmitotic cells rapidly follows the re-assembly of actin specifically at the site of the furrow.

We have previously proposed that the telophase disc determines the position of cleavage by interacting locally with actin and its associated proteins at the cortex of the cell (Andreassen et al., 1991; Margolis and Andreassen, 1993). In support of an essential role for the telophase disc in promulgating cleavage, we have now found that only cells that retain a telophase disc can resume cleavage upon removal of DCB. Further, in such cells, F-actin organizes and cleavage occurs only at the intersection of the telophase disc with the cell cortex. Finally, with increasing time in DCB, the telophase disc can lose association with one side of the cortex. In cells where this has occurred, one always observes a one-sided cleavage occuring only at that portion of the cortex still in contact with the telophase disc.

The mitotic spindle has also been implicated in positioning the site of cleavage (Rappaport, 1986), and the astral microtubule rays of the spindle have been proposed to determine the site of cleavage by distal contact with the cortex. Since both the postmitotic spindle and the telophase disc are retained in cells that remain competent to complete cleavage after removal of DCB, it is possible that the retained spindle is required for cleavage. Various experiments have indicated that the signal for cytokinesis originates from the midzone of the spindle (Rappaport and Rappaport, 1974; Kawamura, 1977). However, since the mammalian spindle is relatively small, it is not apparent that the astral microtubules can reliably contact the cortex to establish the site of cleavage. One possibility, therefore, is that the spindle positions the telophase disc, which then maintains contact with the cortex and determines the site of cleavage. The telophase disc, in this manner, may physically transmit the equatorial signal produced by the spindle.

In conclusion, we find a strong correlation between the presence and position of the telophase disc and furrow formation. Considering that it may now be possible to create a synchronous open cell system for the study of mammalian cell cleavage, it will be of substantial interest to use this system to begin to define the components of the telophase disc and the nature of their interaction with actin, actin associated proteins, and cell cortex elements in the formation of a contractile apparatus.

We are grateful to the following people for providing antibodies used in this study: Dr. J. Kuang for MPM-2 antibodies, Dr. T. Yen for anti-CENP-E antibodies, Dr. R. Kuriyama for anti-MKLP antibodies, Dr. M. Wener for anti–TD-60 antiserum, Dr. M. Kress for anti-human Eg5 antibodies, Drs. Paturle-Lafanechère and D. Job for anti–non-tyrosinated (glu) tubulin antibodies, Dr. J.-C. Courvalin for anti-lamin antibodies, and Drs. S. Schiff and E. Harlow for anti-cyclin B antibodies.

This work was supported in part by grants from the Association pour la Recherche sur le Cancer (ARC), from the National Institutes of Health (GM32022), from the International Human Frontiers of Science Program (RG-513/94 M), and by institutional support from the Commisariat à l'Energie Atomique and the Centre National de la Recherche Scientifique. Ms. Martineau is supported by a doctoral fellowship from La Ligue Contre le Cancer. This is publication no. 280 of the Institut de Biologie Structurale.

Received for publication 17 November 1994 and in revised form 28 March 1995.

References

Andreassen, P. R., D. K. Palmer, M. H. Wener, and R. L. Margolis. 1991. Telophase disc: a new mitotic organelle that bisects telophase cells with a possible role in cytokinesis. *J. Cell Sci.* 99:523–534.

Andreassen, P. R., and R. L. Margolis. 1994. Microtubule dependency of $p34^{cdc2}$ inactivation and mitotic exit in mammalian cells. *J. Cell Biol.* 127:789–802.

Atlas, S. J., and S. Lin. 1978. Dihydrocytochalasin B: biological effects and binding to 3T3 cells. *J. Cell Biol.* 76:360–370.

Aubin, J. E., M. Osborn, and K. Weber. 1981. Inhibition of cytokinesis and altered contractile ring morphology induced by cytochalasins in synchronised PtK2 cells. *Exp. Cell. Res.* 136:63–79.

Bailly, E., M. Dorée, P. Nurse, and M. Bornens. 1989. $p34^{cdc2}$ is located in both nucleus and cytoplasm: part is centrosomally associated at G2/M and enters vesicles at anaphase. *EMBO J.* 8:3985–3995.

Cao, L.-G., and Y.-L. Wang. 1990. Mechanism of the formation of contractile ring in dividing cultured mammalian cells. II. Cortical movement of microinjected actin filaments. *J. Cell Biol.* 110:1089–1095.

Carter, S. B. 1967. Effects of cytochalasins on mammalian cells. *Nature (Lond.).* 213:261–264.

Chaudhary, N., and J.-C. Courvalin. 1993. Stepwise reassembly of the nuclear envelope at the end of mitosis. *J. Cell Biol.* 122:295–306.

Davis, F. M., T. Y. Tsao, S. K. Fowler, and P. N. Rao. 1983. Monoclonal antibodies to mitotic cells. *Proc. Natl. Acad. Sci. USA.* 80:2926–2930.

Earnshaw, W. C., and R. L. Bernat. 1991. Chromosomal passengers: toward an integrated view of mitosis. *Chromosoma.* 100:139–146.

Fenton, B., and D. M. Glover. 1993. A conserved mitotic kinase active at late anaphase-telophase in syncytial *Drosophila* embryos. *Nature (Lond.).* 363: 637–640.

Fishkind, D. J., and Y. L. Wang. 1993. Orientation and three-dimensional organization of actin filaments in dividing cultured cells. *J. Cell Biol.* 123:837–848.

Heidemann, S.R., and M.W. Kirschner. 1975. Aster formation in eggs of *Xenopus laevis*: induction by isolated basal bodies. *J. Cell Biol.* 67:105– 117.

Holloway, S. L., M. Glotzer, R. W. King, and A. W. Murray. 1993. Anaphase is

initiated by proteolysis rather than by the inactivation of maturation-promoting factor. *Cell.* 73:1393–1402.

Hunt, T., F. C. Luca, and J. V. Ruderman. 1992. The requirements for protein synthesis and degradation, and the control of destruction of cyclins A and B in the meiotic and mitotic cell cycles of the clam embryo. *J. Cell Biol.* 116: 707–724.

Kawamura, K. 1977. Microdissection studies on the dividing neuroblast of the grasshopper with special reference to the mechanism of unequal cytokinesis. *Exp. Cell Res.* 106:127–137.

Krishan, A. 1972. Cytochalasin B, time lapse cinematographic studies on its effects on cytokinesis. *J. Cell Biol.* 54:657–664.

Lamb, N. J. C., A. Fernandez, A. Watrin, J.-C. Labbé, and J.-C. Cavadore. 1990. Microinjection of $p34^{cdc2}$ kinase induces marked changes in cell shape, cytoskeletal organization, and chromatin structure in mammalian fibroblasts. *Cell.* 60:151–165.

Margolis, R. L., and P. R. Andreassen. 1993. The telophase disc: its possible role in mammalian cell cleavage. *Bioessays.* 15:201–207.

Nigg, E. A. 1991. The substrates of the cdc2 kinase. *Semin. Cell Biol.* 2:261–270.

Nislow, C., C. Sellitto, R. Kuriyama, and J. R. McIntosh. 1990. A monoclonal antibody to a mitotic microtubule-associated protein blocks mitotic progression. *J. Cell Biol.* 111:511–522.

Nislow, C., V. A. Lombillo, R. Kuriyama, and J. R. McIntosh. 1992. A plus-end-directed motor enzyme that moves antiparallel microtubules *in vitro* localizes to the interzone of mitotic spindles. *Nature (Lond.).* 359:543–547.

Nurse, P., and Y. Bissett. 1981. Gene required in G1 for commitment to cell cycle and in G2 for control of mitosis in fission yeast. *Nature (Lond.).* 292:559–560.

Nurse, P. 1990. Universal control mechanism regulating onset of M-phase. *Nature (Lond.).* 344:503–508.

Paturle-Lafanechère, L., M. Manier, N. Trigault, F. Pirollet, H. Mazarguil, and D. Job. 1994. Accumulation of delta 2-tubulin, a major tubulin variant that cannot be tyrosinated, in neuronal tissues and stable microtubule assemblies. *J. Cell Sci.* 107:1529–1543.

Pines, J., and T. Hunter. 1991. Human cyclins A and B1 are differentially located in the cell and undergo cell cycle-dependent nuclear transport. *J. Cell Biol.* 115:1–17.

Rappaport, R. 1986. Establishment of the mechanism of cytokinesis in animal cells. *Int. Rev. Cytol.* 105:245–281.

Rappaport, R., and B. N. Rappaport. 1974. Establishment of cleavage furrows by the mitotic spindle. *J. Exp. Zool.* 183:115–119.

Rattner, J. B. 1992. Mapping the mammalian intracellular bridge. *Cell Motil. Cytoskeleton.* 23:231–235.

Sanger, J. W., and H. Holtzer. 1972. Cytochalasin B: effects on cytokinesis, glycogen, and ^{3}H-D-glucose incorporation. *Am. J. Anat.* 135:293–298.

Sawin, K. E., K. LeGuellec, M. Philippe, and T. J. Mitchison. 1992. Mitotic spindle organisation by a plus-end-directed microtubule motor. *Nature (Lond.).* 359:540–543.

Sellitto, C., and R. Kuriyama. 1988. Distribution of a matrix component of the midbody during the cell cycle in chinese hamster ovary cells. *J. Cell Biol.* 106: 431–439.

Th'ng, J. P. H., P. S. Wright, J. Hamaguchi, M. G. Lee, C. J. Norbury, P. Nurse, and E. M. Bradbury. 1990. The FT210 cell line is a mouse G2 phase mutant with a temperature-sensitive CDC2 gene product. *Cell.* 63:313–324.

Toyn, J. H., and L. H. Johnston. 1994. The Dbf2 and Dbf20 protein kinases of budding yeast are activated after the metaphase to anaphase cell cycle transition. *EMBO J.* 13:1103–1113.

Vandre, D. D., F. M. Davis, P. N. Rao, and G. G. Borisy. 1984. Phosphoproteins are components of mitotic microtubule organizing centers. *Proc. Natl. Acad. Sci. USA.* 81:4439–4443.

Whitfield, W. G. F., C. Gonzalez, G. Maldonado-Codina, and D. M. Glover. 1990. The A- and B-type cyclins of *Drosophila* are accumulated and destroyed in temporally distinct events that define separable phases of the G2-M transition. *EMBO J.* 9:2563–2572.

Wulf, E., A. Deboben, F. A. Bautz, H. Faulstich, and T. Wieland. 1979. Fluorescent phallotoxin, a tool for the visualization of cellular actin. *Proc. Natl. Acad. Sci. USA.* 76:4498–4502.

Yahara, I., F. Harada, S. Sekita, K. Yoshihira, and S. Natori. 1982. Correlation between effects of 24 different cytochalasins on cellular structures and cellular events and those on actin *in vitro*. *J. Cell Biol.* 92:69–78.

Yen, T. J., D. A. Compton, D. Wise, R. P. Zinkowski, B. R. Brinkley, W. C. Earnshaw, and D. W. Cleveland. 1991. CENP-E, a novel human centromere-associated protein required for progression from metaphase to anaphase. *EMBO J.* 10:1245–1254.

Yen, T. J., G. Li, B. T. Schaar, I. Szilak, and D. W. Cleveland. 1992. CENP-E is a putative kinetochore motor that accumulates just before mitosis. *Nature (Lond.).* 359:536–539.